

The impact of vapor box location on the performance of the multiple effect distillation for seawater desalination technology

Ahmed Abotaleb^a, Abdelnasser Mabrouk^{a,b,*}

^a*Qatar Environment and Energy Research Institute, Hamad Bin Khalifa University, Qatar Foundation, Doha, Qatar, emails: aaboukhlewa@hbku.edu.qa (A. Mabrouk), aabotaleb@hbku.edu.qa (A. Abotaleb)*

^b*College of Science and Engineering, Hamad Bin Khalifa University, Qatar Foundation, Doha, Qatar*

Received 31 May 2020; Accepted 22 November 2020

ABSTRACT

Seawater desalination and water purification is a sustainable solution for arid areas, where the lack of natural potable water is limiting economic growth. Some of the commercial multi-effect distillation (MED) configurations are classified according to the vapor box location with reference to the evaporator tube bundle; whether it is side or back-attached. The lack of technical comparison between the two configurations motivated this work to identify the optimal vapor box location and demister orientation to minimize thermal losses and ensure uniform vapor flow to the next tube bundle. The aim of this study is to perform a computational fluid dynamics (CFD) simulation to compare between two conventional configurations namely the back vapor box (MED-BVB) and the side vapor box (MED-SVB) concerning the thermal losses and vapor flow uniformity as well as to propose internal design modifications specifically in a number of demisters and demister orientation to enhance system performance. MED evaporator of three effects with 25 m³/d is considered for the CFD computational domain and conducted by COMSOL multiphysics. The CFD results showed that, the conventional MED-BVB with one horizontal demister has 49% better vapor uniformity compared to the conventional MED-SVB with three horizontal demisters. However, the modified MED-SVB with three inclined demisters has 45% better vapor uniformity compared to the modified MED-BVB with one inclined demister due to the less swirl flow in the vapor box. Moreover, it was concluded that the modified MED-BVB has a better vapor uniformity and slightly lower thermal loss compared to conventional MED-SVB. Generally, inclining the demister showed better uniform vapor flow in both configurations. On the other hand, the MED-BVB has a 45% lower footprint compared to the MED-SVB. Preference between the two studied configurations would be subjected to the compromise between operational challenges (in case of uneven vapor flow, some tubes would be exposed to a higher amount of vapor flow rate than the design value and accordingly will become overheated) and footprint.

Keywords: Desalination; MED; Thermal losses; CFD; Vapor Route; Vapor uniformity

1. Introduction

Seawater desalination and water purification is a sustainable solution for arid areas, where lack of natural potable water limits economic growth. The Gulf Cooperation Council (GCC) market share of the seawater desalination technologies under the harsh seawater characteristics

(high salinity, elevated temperature, high impurity level, and sometimes red tide) still subjected to the compromise between the energy-efficient reverse osmosis (RO) and the most reliable thermal technology MED. In the GCC region, frequent occurrence of harmful algae blooms (HABs) that may contain toxins that can have passed through the pores of membranes and lead to health problems. Owing to

* Corresponding author.

the uncertainty of RO operation, thermal desalination methods are deemed as the dominant process employed in the desalination market in the Middle East countries, more than 65% of installed capacities however in Qatar, the thermal desalination technologies dominate around 75% of the market, while the rest shared by RO technology [1–3].

Among the thermal desalination technologies, MED operates at relatively lower specific electrical energy consumption compared to RO, where the thermal energy can be ignored at the subsidized tariff and/or at cheap oil price especially at GCC countries. In MED desalination technology, the efficiency and reliability of the falling film evaporation technique have been proofed compared to bulk evaporation [4]. The falling film process, has more advantages than the bulk evaporation, since the tube bundle experience less tendency to heavy scale deposition compared to the immersed tube bundle in the brine pool. In addition, the falling film process has relatively lower seawater charging to the evaporator, and hence lower pumping power.

An innovative solution of integrating the MED system with the heat-driven adsorption desalination (AD) cycle were tested using a pilot plant of 10 m³/d [3]. The AD cycle enables to increase the operating range by lowering the bottom brine temperature under the atmospheric temperature. This in turn allows to add more effect, hence increasing the production of the evaporator compared to the conventional design. The energy and exergy analysis showed comparable consumption to the RO system [3].

It was experimented during the author previous work that, the solar still with floating plate create a thin layer of water and dominate the film evaporation process [5]. In that work, the experimental results showed that the solar still production increased by 30% compared to the conventional bulk evaporation [5]. That film evaporation improvement is mainly due to the available temperature difference between the wall and liquid film. However, there is a limitation and restriction of increasing the temperature difference between the wall and the film to avoid nucleate boiling (bubble formation), which ruptures the film evaporation.

An expression for the maximum temperature difference to avoid bubble formation has been reported [6]. These restrictions motivated us to focus on the thermal losses minimization inside the evaporator so that the temperature difference would increase, and hence improve the film evaporation process. Nevertheless, the main technical challenges of the falling film MED technology are to maintain uniform seawater spraying over tube bundle, to avoid scale formation due to dry patch zones, and to maintain uniform vapor distribution through heating tubes.

Although, on the bench-scale experiments, characterization of the seawater falling film outside the tube can be recorded as well as vapor distribution route. However, for large scale evaporator, numerical simulation is vital. Critical literature review was conducted focusing on the CFD contribution in the field of MED falling film evaporator, which led to identifying the main research gaps on the hydrodynamics and heat/mass transfer aspects [7]. A 2D CFD simulation of the falling film by implementing a volume of fluid (VOF) multiphase model to distinguish liquid and gas phases was developed [8]. The model took into account the effect of viscosity and surface tension and the results showed a

lower conduction thermal resistance at 85°C than at 5°C, which reflects better evaporator performance at higher temperature [8].

On the other hand, while the vapor sweeping from the tube bundle sides, it will move around the tubes and intersect with the seawater falling film. The vapor streams may deflect the falling film away, which causes incomplete wetting for the lower tubes. Based on the tube bundle arrangement and the critical deflection angle, Lorenz et al. [9] developed the maximum allowable vapor crossflow velocity to avoid deflection phenomena in the MED evaporator.

The effect of a new baffle configuration based on CFD simulation showed a minimum brine carryover, and lower demister pressure drop [10]. A comparison between four-different designs of the flash chamber of MSF plant was performed in which, the demister located at the middle of the chamber has a better performance in terms of higher separation efficiency with relatively lower demister pressure drop [11].

Several MED evaporator configurations have been installed in the desalination industry either based on a cross tube or long tube orientation [12]. CFD simulation of the vapor route for the two conventional MED configurations were performed by the authors [12] and the results showed the superiority of the long tube MED in terms of better vapor uniformity and lower footprint. In this study, the evaporator tube bundle contributed to almost 88% of the thermal losses, which encourages the researchers and engineers to focus on minimizing the thermal losses within the evaporator tube bundle.

Another two commercial MED evaporators were installed based on the location of the demister whether it is in the evaporator or back-side [13]. In this CFD study, the 60° triangle pitch showed better performance for the side demister (MED-SD) evaporator, while the 30° triangle pitch arrangement fits the back demister (MED-BD) evaporator. The vapor velocity distribution at the tube sheet of the MED-BD evaporator has a better uniform flow [13].

Nevertheless, two commercial large scale MED desalination plants are classified according to the vapor box location with reference to the evaporator tube bundle; whether it is back or side-attached. Fig. 1a shows top view sketch for one of the two MED configurations in which the evaporator consists of N effects and namely the back vapor box (MED-BVB). This layout shows that, the vapor box location is in-between two subsequent effects, where the generated vapor from the first effect is routed to the second effect. The length of the vapor box is equal to the tube length for sake of maintenance, while the width is determined by the tube bundle width in addition to the demister length. Fig. 1b shows the top view sketch of another MED configuration consists of N effects and namely the side vapor box (MED-SVB). This layout shows that, the first effect is divided into two equal cells, where the vapor box location is in-between. However, for the second effect, the vapor box is divided into two equal parts, where the tube bundle is located in-between. The first effect vapor box length is equal to the tube length for sake of maintenance, while the width is determined also by the tube bundle width in addition to demister length. For the second effect, each part of the vapor box has a length equal to the tube and width of cell A or B .

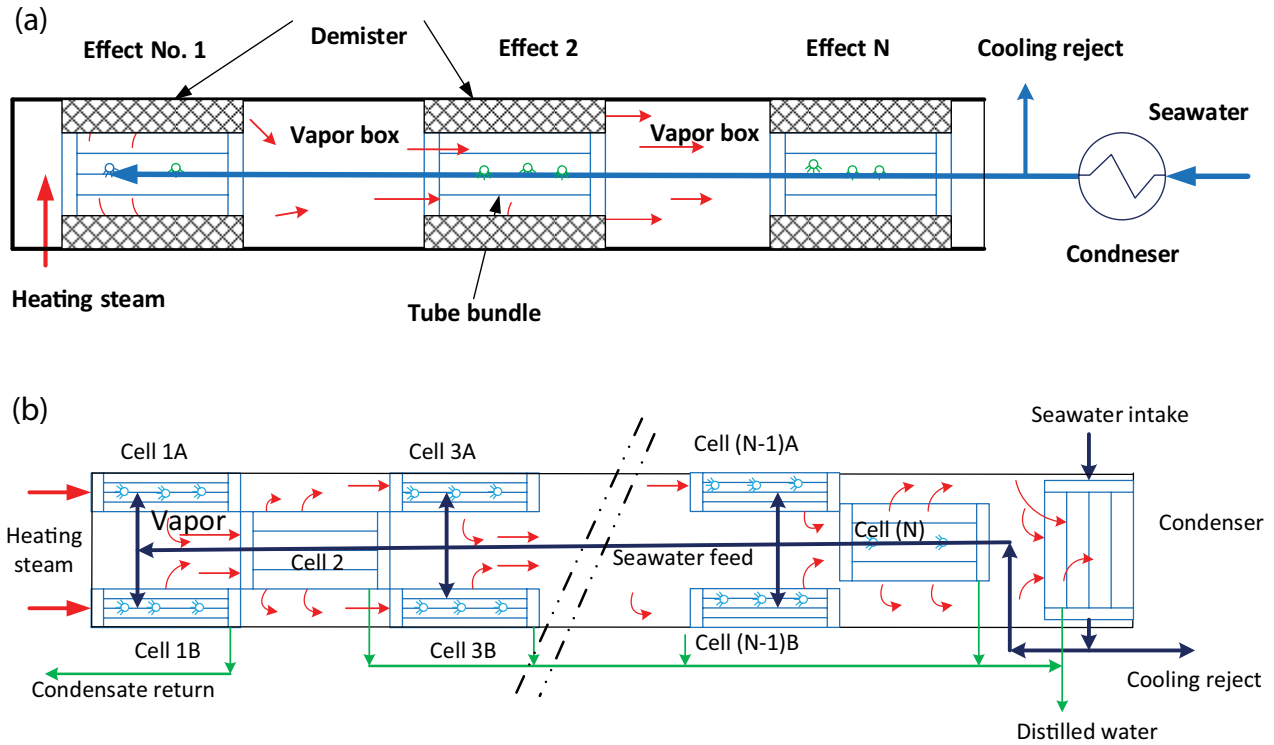


Fig. 1. Top view of conventional evaporator layout (a) back vapor box (MED-BVB), Taweelah, UAE and (b) side vapor box (MED-SVB), Rass Laffan, Qatar.

The lack of a technical comparison between the two configurations motivated this work to identify the pros and cons of attaching the vapor box either at the backside (Fig. 1a) or at the side of the tube bundle (Fig. 1b).

The aim of this study is to perform a CFD simulation of the vapor route within the MED-BVB and the MED-SVB configurations concerning the thermal losses and vapor flow uniformity. The vapor route temperature, pressure drop, and velocity profile will be identified and used to calculate the thermal losses within the evaporator as well as the vapor flow uniformity at the inlet of the next tube bundle. This study will address and propose an internal design modifications specifically in a number of demisters and demister orientation to enhance system performance.

2. Methodology

2.1. Model domain, mathematical model

Steady-state two-dimensional and three-dimensional computational fluid dynamic (CFD) models were built using COMSOL multiphysics for one effect of the MED evaporator. To ensure accurate results and optimum computation time we used 2D and 3D models. Since the pattern of the evaporation and pressure within the tube bundle does not change in the longitudinal direction (tube length). Therefore, 2D models are valid to present the pattern in the cross-section, while the pattern of the pressure drop changes in both crosses (x -direction), vertical (y -directional), and (z -directional) so that 3D models are essential to check the generated vapor from tube bundle passing by demister then vapor box

until reaching next tube bundle. The modeling approach has been developed following these assumptions:

- Steady-state
- Weakly-compressible Newtonian flow
- Demister as porous media
- The model is under vacuum pressure
- Saturated steam flow inlet to demister and vapor box at 50°C
- Local velocity inlet vapor flow

The computational domain for vapor flow through vapor box has been modeled in three-dimensional platform using $k-\epsilon$ flow package integrated with the effect of heat transfer. The main governing equations are Navier–Stokes for the conservation of momentum and the continuity equation for conservation of mass. The standard $k-\epsilon$ equations were selected due to its robustness and relatively low computational time compared to other turbulence model as listed in literature [10–17]. The physics behind the model are extracted from the authors’ latest work [12,13], where below are the main equations used in the model:

Continuity equations:

$$\frac{\partial}{\partial t}(\rho_m) + \nabla(\rho_m \vec{v}_m) = \dot{m} \quad (1)$$

Mass-averaged velocity:

$$\vec{v}_m = \frac{\sum_{k=1}^n \alpha_k \rho_k \vec{v}_k}{\rho_m} \quad (2)$$

Density mixture:

$$\rho_m = \sum_{k=1}^n \alpha_k \rho_k \quad (3)$$

Momentum equation for each phase:

$$\frac{\partial}{\partial t} (\rho_m \bar{v}_m) + \nabla (\rho_m \bar{v}_m \bar{v}_m) = -\nabla p + \nabla [\mu_m (\nabla \bar{v}_m + \nabla \bar{v}_m^T)] + \rho_m \bar{g} + \bar{F} + \nabla \left(\sum_{k=1}^n \alpha_k \rho_k \bar{v}_{dr,k} \bar{v}_{dr,k} \right) \quad (4)$$

Viscosity mixture:

$$\mu_m = \sum_{k=1}^n \alpha_k \mu_k \quad (5)$$

Secondary phase drift velocity:

$$\bar{v}_{dr,k} = \bar{v}_k - \bar{v}_m \quad (6)$$

Energy equation:

$$\frac{\partial}{\partial t} \sum_{k=1}^n (\alpha_k \rho_k E_k) + \nabla \sum_{k=1}^n (\alpha_k \bar{v}_k (\rho_k E_k + p)) = \nabla (k_{\text{eff}} \nabla T) + S_E \quad (7)$$

where k_{eff} is the effective conductivity ($k + k_t$), where k_t is the turbulent thermal conductivity. The first term on the right-hand side represents energy transfer due to conduction. S_E includes any other volumetric heat sources. For a compressible phase, and $E_k = h_k$ for an incompressible phase, where h_k is the sensible enthalpy for phase k .

$$E_k = h_k - \frac{p}{\rho_k} + \frac{v_k^2}{2} \quad (8)$$

Relative velocity:

$$\bar{v}_{pq} = \bar{v}_p - \bar{v}_q \quad (9)$$

The relative velocity (also referred to as the slip velocity) is defined as the velocity of a secondary phase (p) relative to the velocity of the primary phase (q). Volume fraction of the secondary phase. From the continuity equation for secondary phase p , the volume fraction equation for secondary phase p can be obtained:

$$\frac{\partial}{\partial t} (\alpha_p \rho_p) + \nabla (\alpha_p \rho_p \bar{v}_m) = -\nabla (\alpha_p \rho_p \bar{v}_{dr,p}) \quad (10)$$

2.2. Boundary conditions

The model boundary conditions are presented in Table 1. The heating steam is flowing to the first tube bundle at 53°C and will be condensed inside the tubes and transfer the latent to the falling seawater around the tubes. Only some portion of the falling film converted as vapor at 50°C, while the rest (brine) is collected in the brine sump at relatively higher temperature to consider the boiling point elevation. 620 tubes are arranged in a triangular tube pitch. The outside tube diameter is 25.4 mm and 1 m in length. Demister thickness is 0.15 m. The effect of a number of demisters and demister inclination on the thermal losses and vapor uniformity are also investigated at different recovery ratio (the ratio between the amounts of generated vapor to the seawater falling film) of 11%, 22%, and 33% to consider a wide range of vapor velocity in practical MED desalination plants.

Fig. 2a shows the MED-BVB dimensions in the meter. Because of symmetrical geometry, only half of the domain was considered to save computation time. In this configuration, the vapor box location is in between two effects to facilitate vapor movement from one effect to another. The generated vapor coming out from tube bundle sides

Table 1
Boundary conditions for one effect of MED evaporator

Parameter	Value	unit
Falling film flow rate (feed seawater)	3	m ³ /h
Feed temperature	42	°C
Feed salinity	45	g/L
Inlet vapor temperature	53	°C
Generated vapor temperature	50	°C
Recovery ratio	11–33	%
No. of demisters	1, 2, and 3	
Demister orientation	Horizontal and inclined	
No. of tubes	620	
Tube diameter (OD)	25.4	mm
Tube length	1	m
Vapor box length	1	m
Tube bundle height	0.7	m
Tube bundle width	2	m

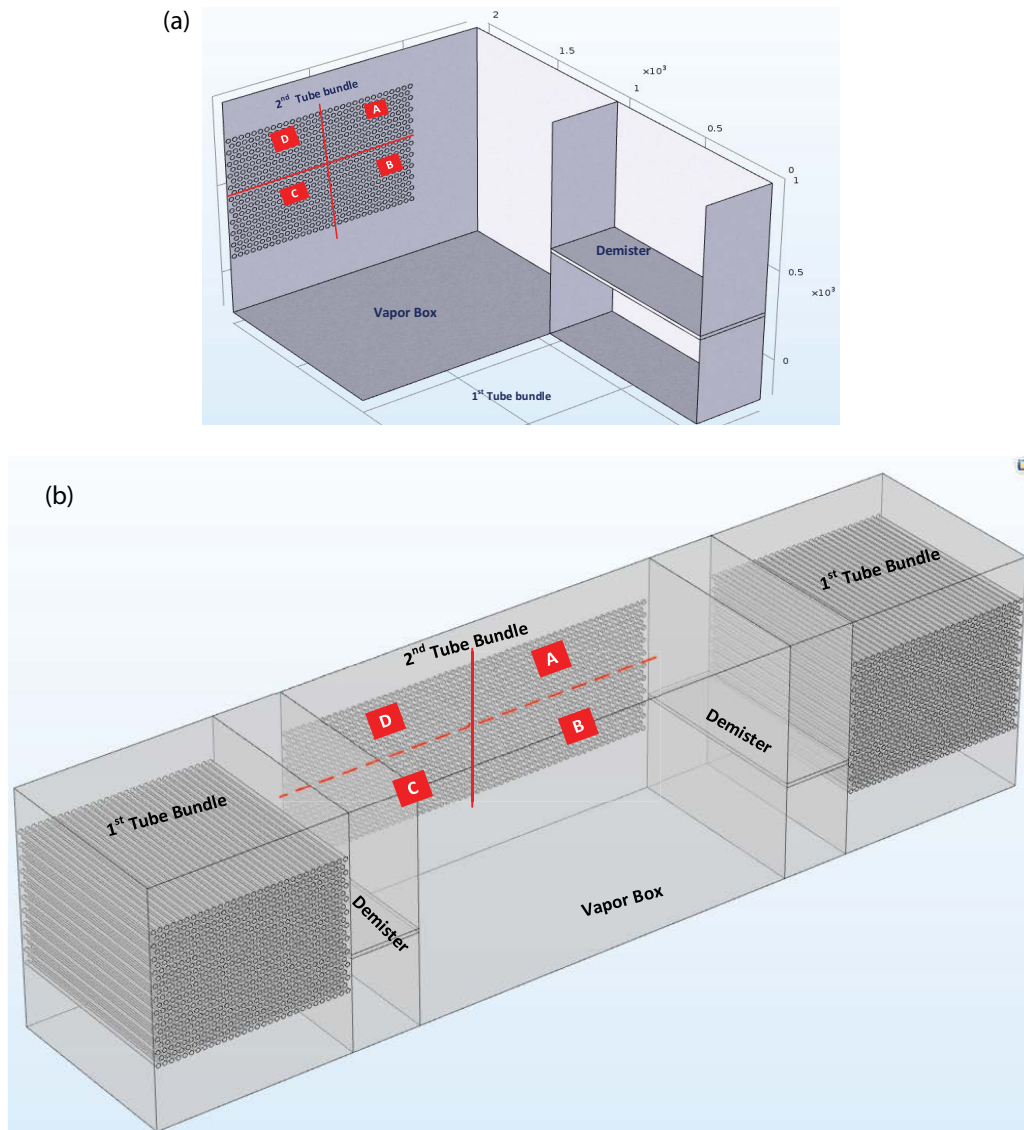


Fig. 2. Hypothetical segments to determine the uniformity of vapor velocity at the entrance of the second tube bundle for (a) MED-BVB and (b) MED-SVB.

flow through horizontal demisters to be accumulated in the vapor box and then routed to tube sheet of the next effect. Fig. 2b shows the MED-SVB dimensions in the meter. In this configuration, the vapor box location is in between two cells, where each cell is half of the first effect. The generated vapor flow from cells passed through horizontal multi demisters to be accumulated in the vapor box and then routed to tube sheet of the next effect.

For both configurations, MED-BVB and MED-SVB, the calculated outlet boundary conditions at the side of the evaporator tube bundle are used as input boundary conditions (pressure, velocity, and temperature) to the demister. Since the velocity profile of the swept vapor from the evaporator bundle, massively affect the uniformity at the inlet demister and accordingly, the vapor box before approaching the next evaporator. Therefore, the typical local vapor velocity profile at the evaporator exit side

is applied as an inlet boundary to the second segment as shown in Fig. 3. The MED cell height is 1.2 m distributed as (0.2 m for falling film liquid distribution, 0.7 evaporator tube bundle, and 0.3 m as a liquid sump for brine). The upper demister is located at a height of 0.7 m, however, the lower demister is located at 0.3 m.

The local vapor velocity reaches up to 40 m/s, which reflects a practical challenge in commercial desalination plants. In fact, this high velocity has a negative impact on system mechanical stress and tube support as well as one of the main reasons for creating swirl flow in the vapor box.

2.3. Mesh size and resolution

For sake of higher mesh resolution and ensuring accurate findings, several types of mesh elements have been used in this study including prism, tetrahedral, triangular,

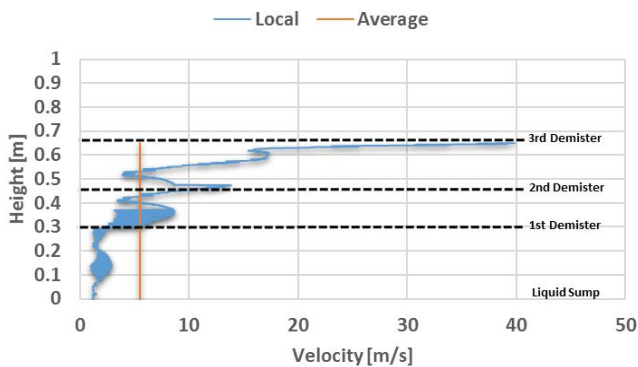


Fig. 3. Vapor velocity distribution through sides of the tube bundle “horizontal demister”.

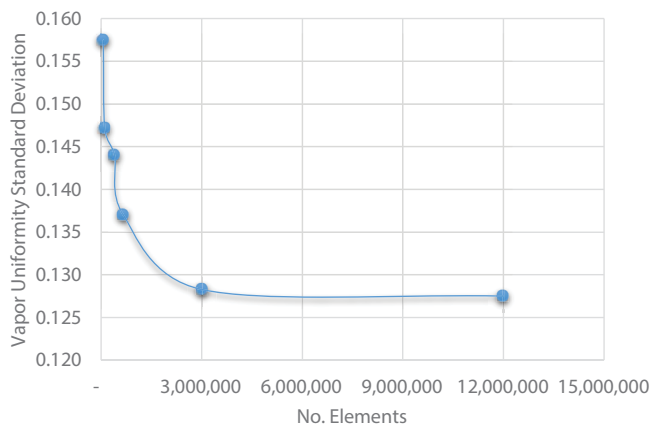


Fig. 4. Criteria selection for number of mesh elements [12,13].

and quadrilateral. The vapor uniformity standard deviation is calculated at different mesh sizes as shown in Fig. 4 ranging from 1,000 up to 12 million number of elements. Vapor uniformity reach almost constant and the curve becomes flat at almost 3 million elements, but it consumes long time. Tradeoff between computation time and high resolution always exist. Therefore, 3 million elements was selected in this study. In addition, the termination criteria for the solver was adjusted at 10^{-5} .

2.4. CFD model validation

It's worth mentioning that, the CFD model results has been verified based on overall mass and heat balance against the Visual Design Simulation (VDS) program [18,19] and presented in the author previous work [12,13]. The VDS program is a well know process design software developed by the author and used for desalination technologies design and system evaluation. This process design tool has already been validated against real desalination plants and many papers were published utilizing this software [18,19]. In this study, MED pilot plant of $24 \text{ m}^3/\text{d}$ with three effects is considered as a case study. The detailed design of the pilot plant is carried out using process design program (VDS) [18,19]. The evaporator heat transfer area and dimension are calculated accordingly using VDS to be used as a

fixed domain for CFD simulation. Using the data of Table 1, the 2D CFD model for the evaporator bundle calculated the amount and temperature of generated vapor as well as exit brine temperature. On the other hand, the CFD model for two-phase flow has been validated for predicting the pressure drop in the tube bundle using published numerical correlation, which is presented in the author previous work; Eqs. (1)–(11) [12]. The CFD numerical model is based on Euler–Euler physics, where the homogeneous void fraction is a function of the recovery ratio, liquid, and vapor physical properties and each phase velocity. Finally, the demister pressure drop calculated from the CFD model was verified against empirical equations based on real experiments from a manufacturer [20], detailed equations are presented in the author previous work; Eqs. (12)–(17) [12].

2.5. Calculation of the average velocity at the tube sheet

Fig. 2a shows the hypothetical four segments (A, B, C, and D) for MED-BVB to calculate the local velocity in each segment and then to identify the deviation compared to the whole tube sheet average velocity. The average approaching velocity at the tube sheet is calculated as 5 m/s at 11% process recovery.

Fig. 2b shows the hypothetical four segments (A, B, C, and D) for MED-SVB to calculate the local velocity in each segment and then to identify the deviation compared to the whole tube sheet average velocity. The average approaching velocity at the tube sheet is calculated as 5 m/s at 11% process recovery ratio. Eq. (11) below reflect the standard deviation formula used in this study:

$$\sigma = \sqrt{\frac{\sum (x_i - \mu)^2}{N}} \quad (11)$$

where σ is the population standard deviation; N is the size of the population; x_i is each value from the population; μ is the population mean.

3. Results and discussion

3.1. Analysis of the MED-SVB configuration

The developed CFD model predicts the velocity distribution as shown in Figs. 5a and b at different demister number (one and three), respectively. Moreover, Fig. 5c shows that, the flow uniformity standard deviation increases as the process recovery ratio increases. This is because of a high amount of vapor was generated within the tube bundle and this amount has to pass through the same passage from the bundle side, crossing demister and through the vapor box. At high vapor velocity, the intensity of the swirled flow increases and due to change in the directions that drive the vapor to lose its uniformity at the tube sheet. The better vapor uniformity is obtained when three demisters is used compared to one demister as shown in Fig. 5c.

Furthermore, Fig. 5d shows the total thermal losses increase as the process recovery ratio increases due to the increase of the friction losses encountered. The three demisters show slightly higher thermal losses, followed by one demister. This is because of implementing multi demisters,

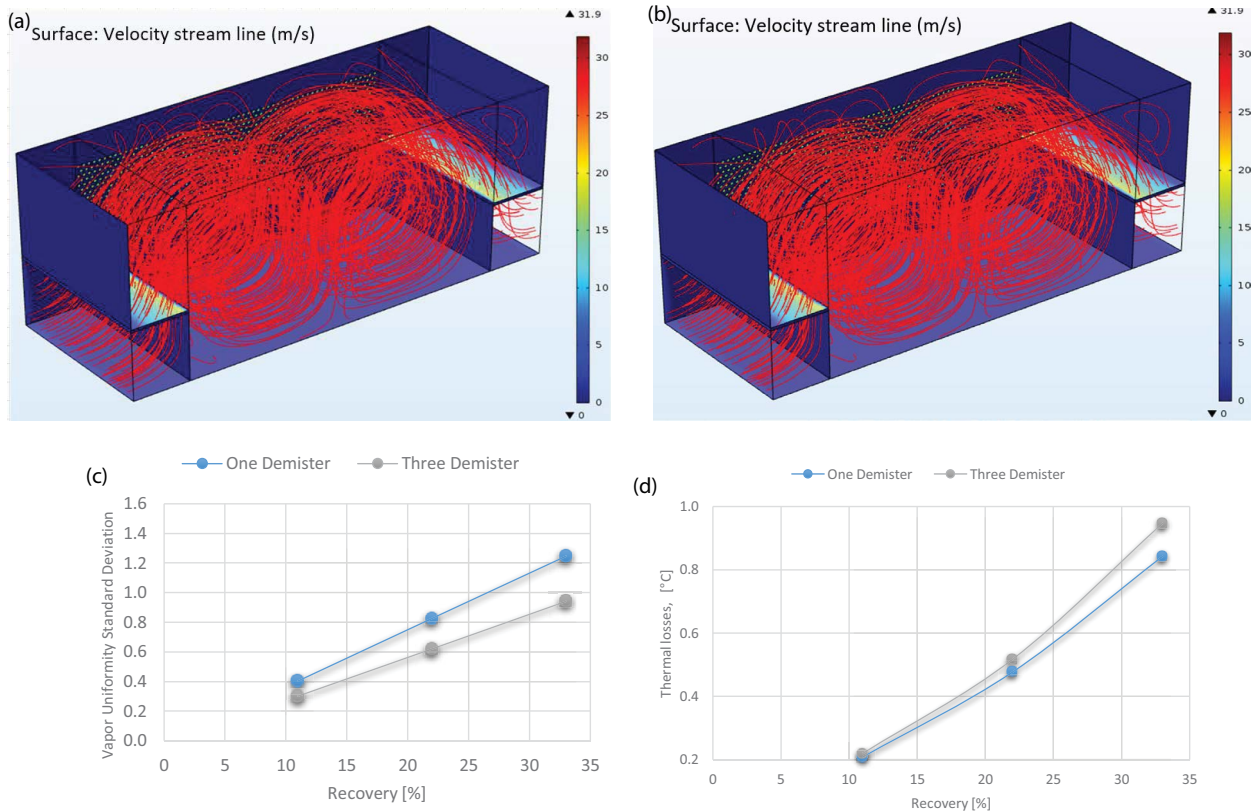


Fig. 5. MED-SVB (a) one, (b) three horizontal demisters, (c) vapor uniformity, and (d) thermal losses of MED-SVB horizontal demister configuration.

which create a narrow passage between the top and middle and between the middle and the lower demister. These passages have un-equal cross-sectional areas, which creates imbalance vapor velocity and accordingly more swirl flow in the vapor box.

The developed CFD model predicts the velocity distribution as shown in Figs. 6a and b at a different number of demisters (one and three), respectively, and 45° inclination as the effect of implementing an inclined demister orientation is reflected. The obtained results showed that, the vapor flow standard deviation increases at a higher process recovery ratio regardless of the demister number as shown in Fig. 6c. The better vapor flow uniformity is obtained when three demisters are used followed by one demister, following the same order of the horizontal configuration.

Moreover, Fig. 6d shows that the thermal losses increase as the process recovery ratio increases due to the increase of the friction losses encountered due to the high vapor velocity and there is no much difference in thermal losses between one-inclined demister and three-inclined demister. Therefore, it could be concluded from Fig. 6 that implementing three inclined demisters is superior to one demister with respect to this configuration.

Fig. 7a shows that, the three-inclined demister creates a lower standard deviation of the vapor velocity than three-horizontal demister, which is the conventional configuration. This is because the inclination of the demister creates a larger passage of vapor flow before approaching

the vapor box as a result a smooth change of direction was obtained. This is in turn allows a large exposure area of the tube sheet to the vapor flow, which creates a better uniform approach velocity. Furthermore, Fig. 7b shows that, inclining the demister has a positive effect on the thermal losses encountered in the vapor route as the three-inclined demister showed a slightly lower thermal loss than the three-horizontal demister.

3.2. Analysis of the MED-BVB configuration

On the other hand, applying the same concept of multi-demisters and inclination has been checked also on a conventional MED system. This configuration called MED-back vapor box (MED-BVB). The developed CFD model predicts the velocity distribution as shown in Figs. 8a–d at a different number of demisters (one and three) and demister orientation. The inclined demisters are at 45° angle.

Fig. 9a shows that, the flow uniformity standard deviation increases as the process recovery ratio increases. This is because of a high amount of vapor was generated within the tube bundle and this amount has to pass through the same passage from the bundle side, crossing the demister, and through the vapor box. At high vapor velocity, the intensity of the swirled flow increases and due to change in the directions that drive the vapor to lose its uniformity at the tube sheet. The better vapor uniformity is obtained when one demister is used compared with three demisters

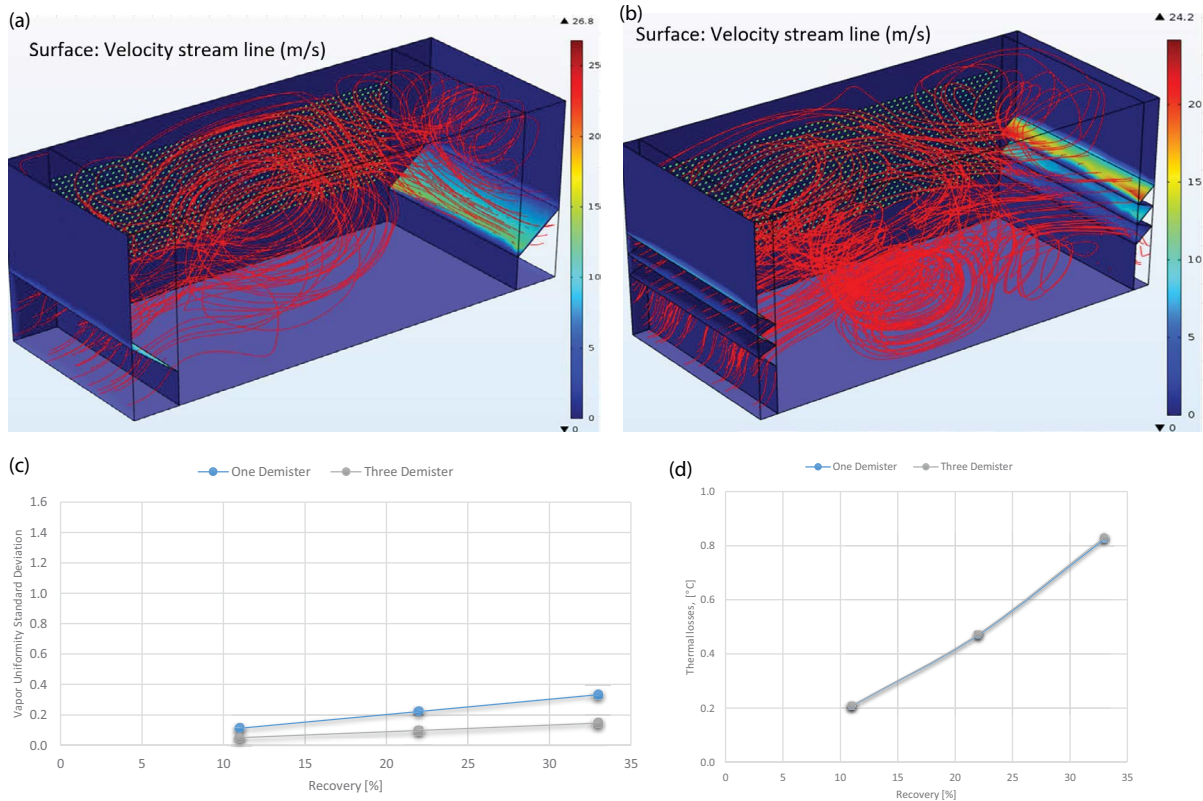


Fig. 6. MED-SVB (a) one, (b) three inclined demisters, (c) vapor uniformity, and (d) thermal losses of MED-SVB inclined demister configuration.

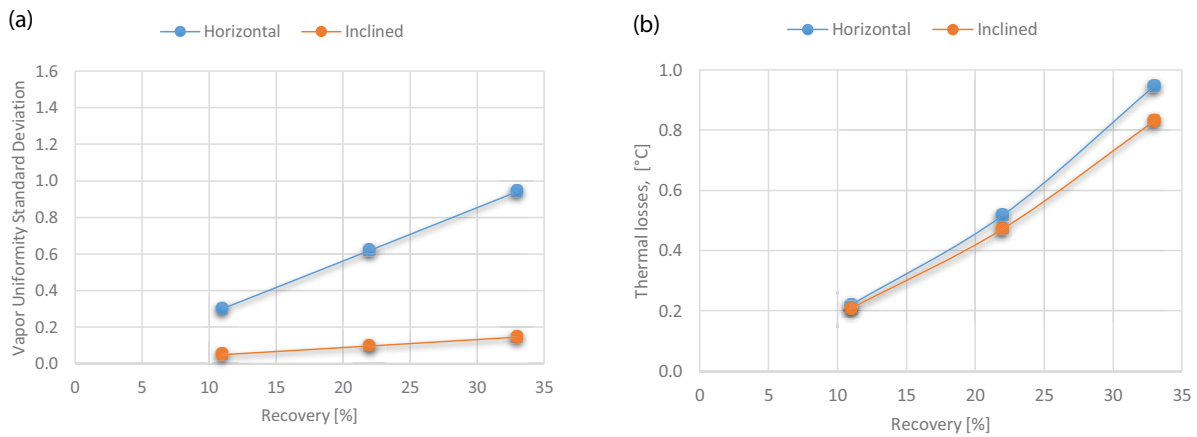


Fig. 7. (a) Vapor velocity standard deviation comparison for three-demister MED-SVB and (b) MED-SVB thermal losses comparison, three-demister.

as shown in Fig. 9a. Using three demisters with the same area of one demister dictated a shorter demister width compared to one demister. These narrow passages create an imbalanced mass flow among demisters. This in turn creates a swirl flow in the vapor box, which causes a non-uniform velocity distribution at the following tube sheet.

Furthermore, Fig. 9b shows that, the total thermal losses increase as the process recovery ratio increases due to the increase of the friction losses encountered. The three

demisters show higher thermal losses, while the lower thermal losses are obtained at one demister. This is because of implementing multi demisters, which create a narrow passage between the first and middle and between the middle and the lower demister. These passages have unequal cross-sectional areas, which creates imbalance vapor velocity and accordingly more swirl flow in the vapor box.

Fig. 10a shows the effect of implementing an inclined demister. The obtained results showed that the vapor flow

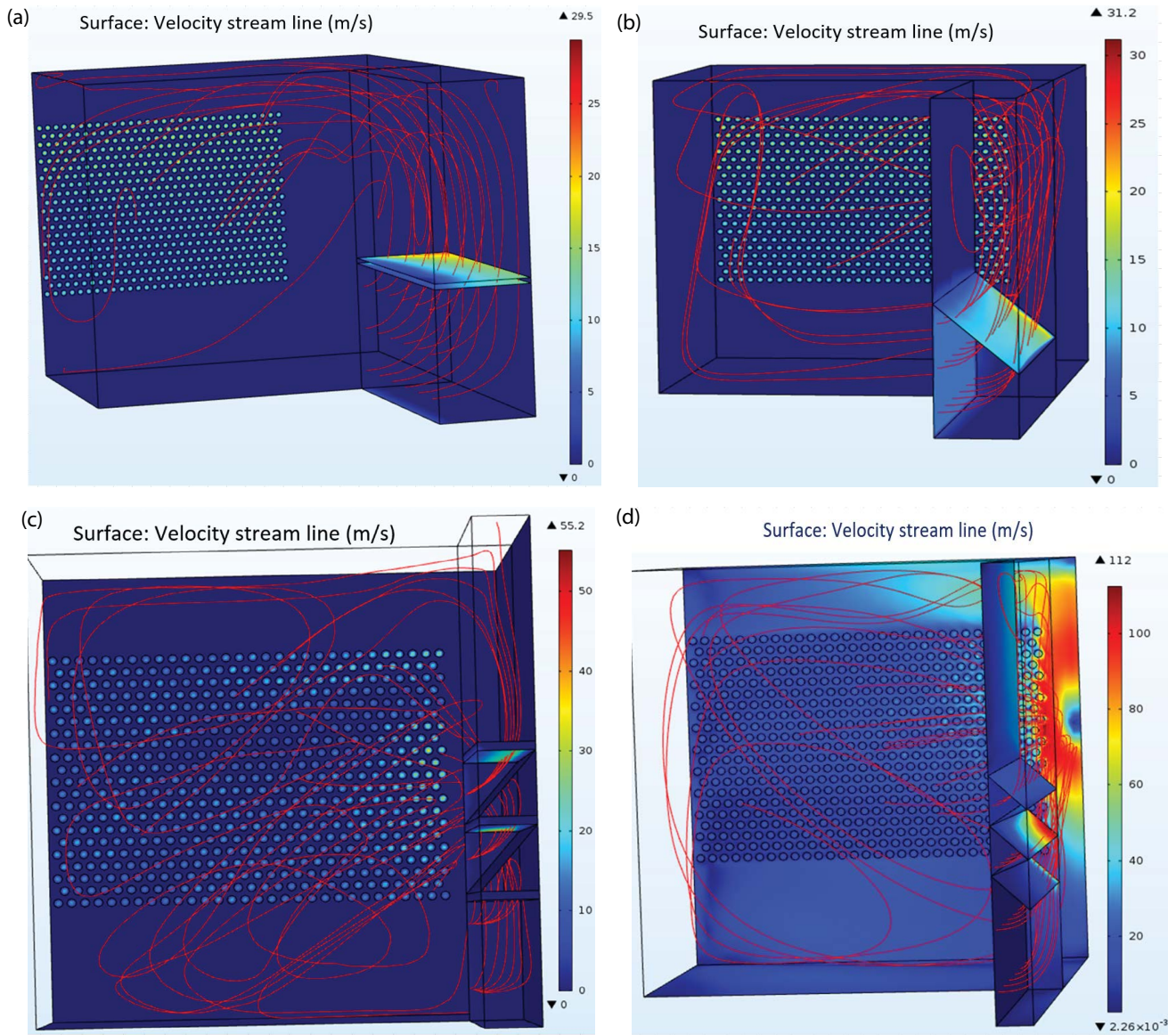


Fig. 8. MED-BVB single demister (a) horizontal and (b) inclined; three demisters (c) horizontal and (d) inclined.

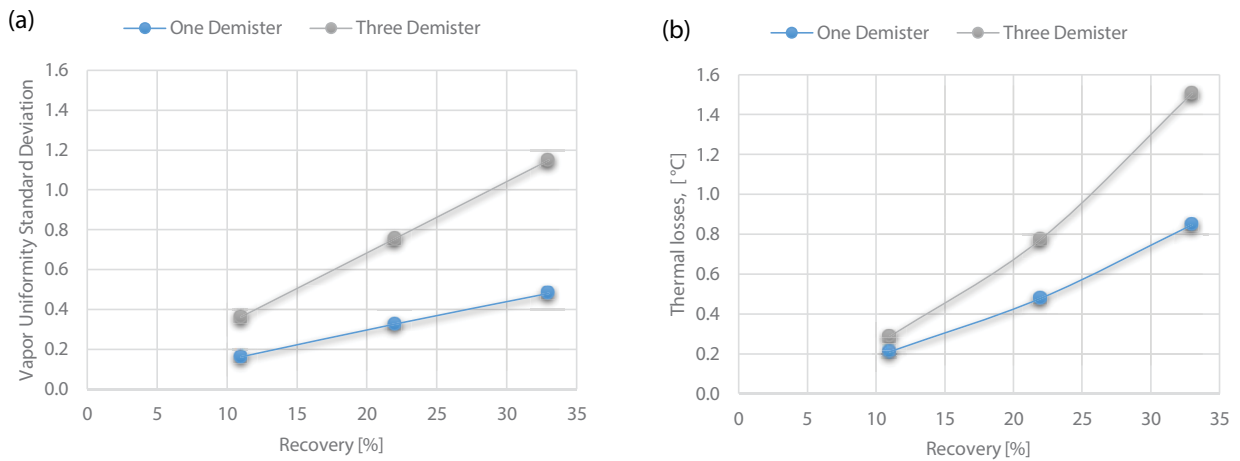


Fig. 9. MED-BVB (a) vapor uniformity and (b) thermal losses of horizontal demister configuration.

standard deviation increases at a higher process recovery ratio regardless of the demister number as shown in Fig. 10a. The better vapor flow uniformity is obtained when one demister is used compared to three demisters. In fact, three demisters with the same area of one demister dictated a shorter demister width compared to one demister. However, these narrow passages create an imbalanced mass flow rate and accordingly more swirl flow in the vapor box, which ends with un-uniform velocity distribution at the tube sheet.

Moreover, Fig. 10b shows that the thermal losses increase as the process recovery ratio increases due to the increase of the friction losses encountered due to the high vapor velocity. The higher thermal losses are calculated at three inclined demisters, while the lower thermal losses are obtained at one inclined demister. This is because of implementing multi demisters creates a narrow passage between the top and middle and between the middle and the lower demister. These passages have un-equal cross-sectional areas, which creates imbalance vapor velocity and accordingly more swirl flow in the vapor box. It could be concluded from Figs. 9a and b; 10a and b that implementing one demister is superior to multi demisters.

Fig. 11a shows that the one inclined demister creates a lower standard deviation of the vapor velocity than one horizontal demister. This is because of inclining the demister creates a larger passage of vapor flow before approaching the vapor box as a result a smooth change of direction was obtained. This in turn allows a large exposure area of the tube sheet to the vapor flow, which creates a better uniform approach velocity. On the other hand, Fig. 11b shows that inclining the demister has no influence in the thermal losses encountered in the vapor route since most of the thermal losses (85%) occurred in the tube bundle and only 7% in the demister while 8% in the vapor box [13].

3.3. Comparison between MED-SVB and MED-BVB

The conventional configurations MED-BVB with one horizontal demister and the MED-SVB with three horizontal demisters are compared. Figs. 12a and b reflect the vapor uniformity and thermal losses for both configurations, respectively. At 33% process recovery ratio, the MED-BVB configuration shows a 49% better vapor uniformity,

this because of the formation of two big swirls in MED-SVB due to the nature of the freely flowing flow through three horizontal demisters creating vortex flow in the empty area (vapor box) then reunion again to flow axially in next tube bundle (Fig. 5b). Moreover, Fig. 12c shows 2D cross-section at 15 mm distance from the next tube bundle, where the two big swirls formed and maximum velocity recorded at 34 m/s. Those two big swirls mainly formed from the top demister, where most of the vapor generated and sweeping to vapor box then to next tube-bundle.

On the other hand, the one horizontal demister for MED-BVB configuration showed almost smooth flow with a minor vortex (Fig. 8a) and Fig. 12d, where 2D cross-section at 15 mm distance from next tube bundle shows minor vortices with maximum velocity reported at 21.9 m/s. In fact, the swirl induces an increase in the entrainment rate and a decrease in the axial flow velocity. Accordingly, the formation of those vortexes would consume pressure energy and increase thermal losses. Thus, the MED-BVB has 10% less thermal losses compared to MED-SVB as shown in Fig. 12b.

Fig. 12e shows that, the MED-BVB has 37% lower footprint of MED-SVB, this because of the MED-SVB vapor box is located between two cells within the same length of the current effect and have the same width of the next effect, which increase the evaporator width compared to MED-BVB as shown in Fig. 1.

It could be concluded from the previous sections that, the MED-SVB with three inclined demisters and the MED-BVB with one inclined demister have a better vapor uniformity. Accordingly, Fig. 13a shows that the MED-SVB configuration has a 45% better vapor uniformity. This could be justified because of inclining the demisters ensured a larger area for generated vapor and accordingly almost uniform flow through a demister to vapor box. The formation of swirls in this configuration has dramatically reduced from two big swirls as shown in Fig. 5b to only one small swirl referring to Fig. 6b. Moreover, Fig. 13c shows 2D cross-section at 15 mm distance from the next tube bundle, where the only big swirl formed and maximum velocity recorded at 25 m/s. This swirl mainly formed from the top demister, where most of the vapor generated and sweeping to vapor box then to next tube-bundle. Moreover, Fig. 13d, where 2D cross section at 15 mm distance from the next

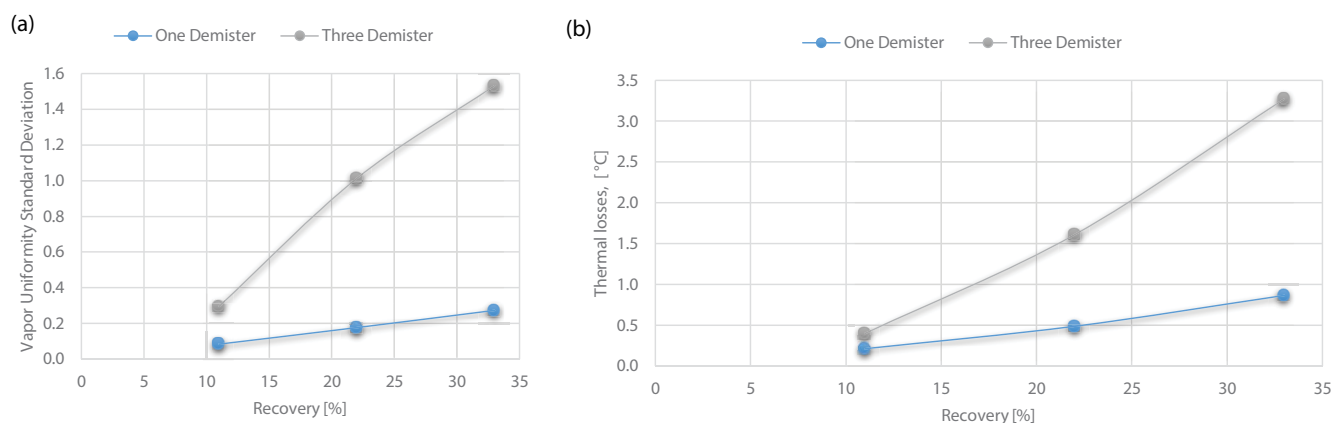


Fig. 10. MED-BVB (a) vapor uniformity and (b) thermal losses of inclined demister configuration.

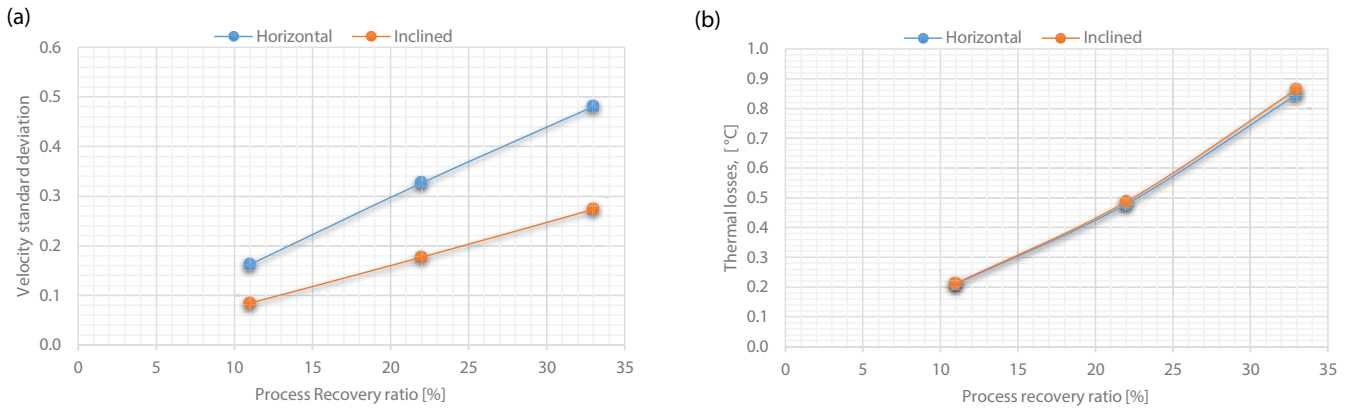


Fig. 11. MED-BVB (a) vapor velocity standard deviation comparison and (b) thermal losses comparison, one demister.

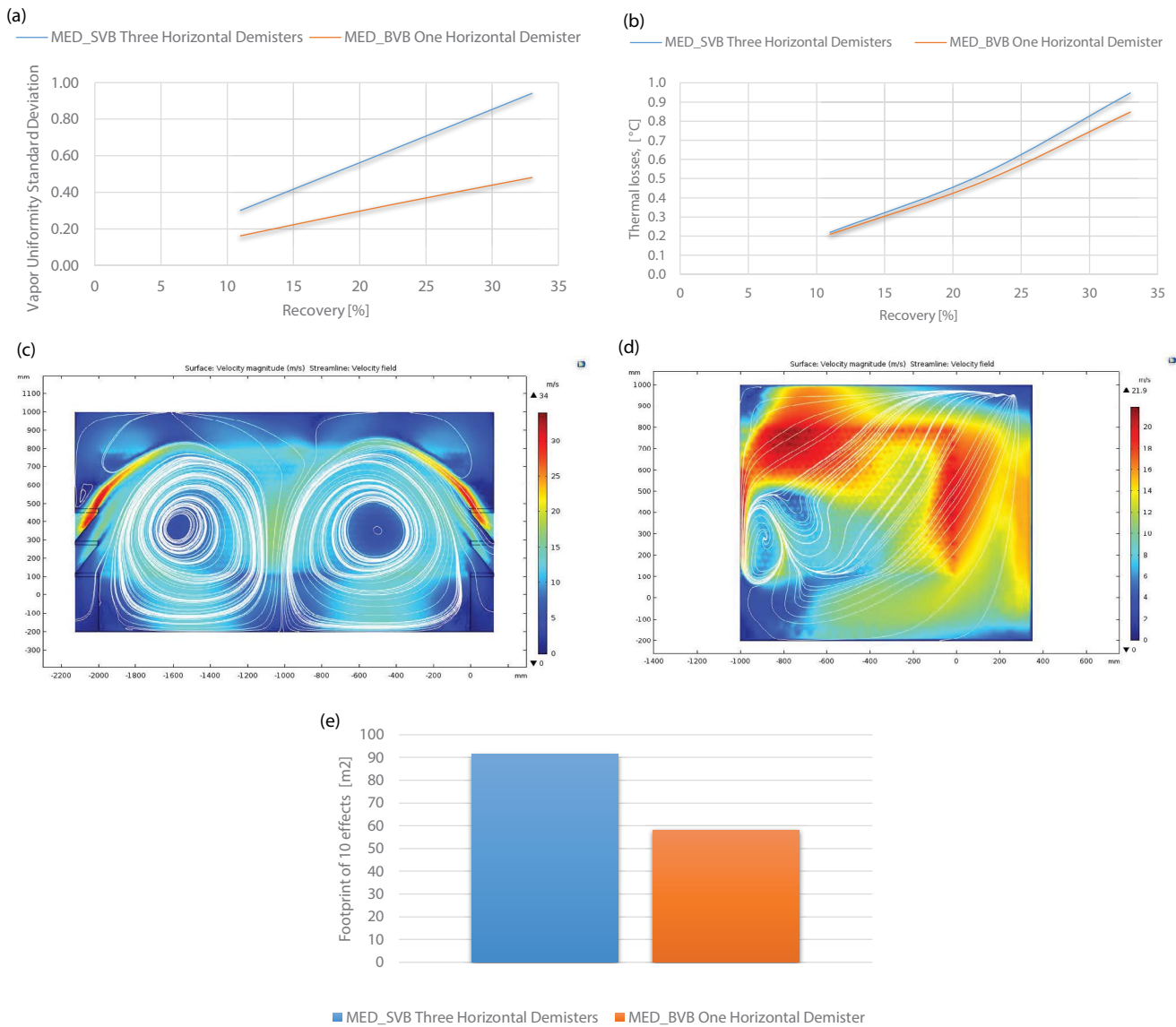


Fig. 12. (a) Vapor uniformity, (b) thermal losses of MED-SVB three horizontal demisters and MED-BVB one horizontal demister, (c) MED-SVB three horizontal demisters, (d) MED-BVB one horizontal demister 2D cross-section at 15 mm distance from next tube bundle, and (e) footprint of the MED-SVB three horizontal demisters and MED-BVB one horizontal demister.

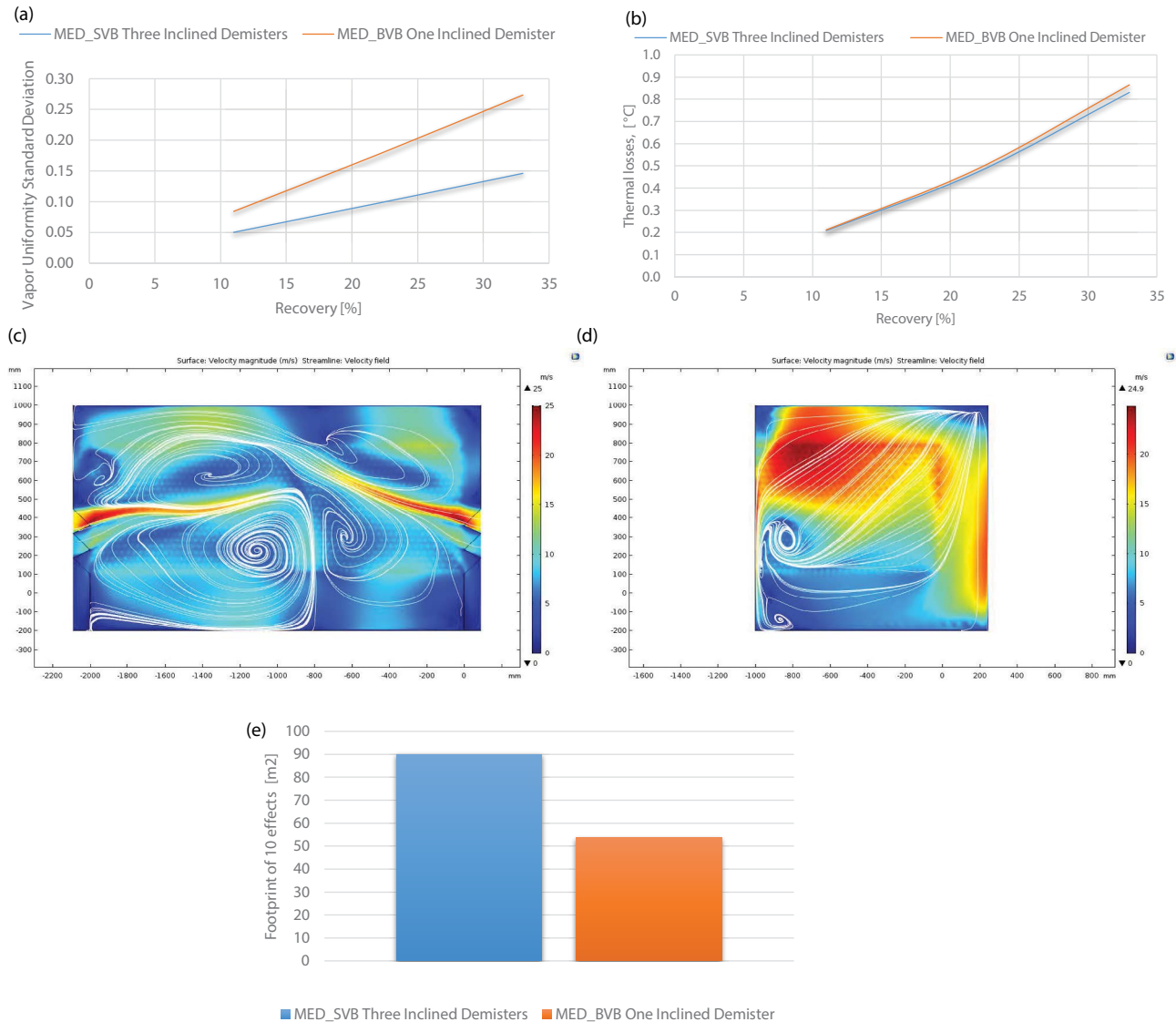


Fig. 13. (a) Vapor uniformity, (b) thermal losses of final comparison between MED-SVB three inclined demisters and MED-BVB one inclined demister, (c) MED-SVB three inclined demisters, (d) MED-BVB one inclined demister 2D cross-section at 15 mm distance from next tube bundle, and (e) footprint between comparison between MED-SVB three inclined demisters and MED-BVB one inclined demister.

tube bundle shows minor vortices with maximum velocity reported 24.9 m/s. On the other hand, Fig. 13b shows there was not significant difference in the generated thermal losses in both configurations.

The MED-SVB with three inclined demisters configuration has a 40% higher footprint compared to MED-BVB with one inclined demister because of the vapor box of the MED-SVB is located between two cells with the same length of the current effect and have the same width of the next effect, which increases the evaporator width compared to MED-BVB as shown in Fig. 1.

From Figs. 12 and 13, we could conclude that, conventional MED-BVB configuration has a better vapor uniformity and slightly lower thermal losses within the vapor route compared to the conventional MED-SVB configuration. However, by applying the proposed inclining demister, the

CFD results showed a better uniform vapor flow in both configurations compared to conventional designs. Inclining the demisters showed a superior of the MED-SVB configuration as it showed better vapor flow due to the wide passage resulted in less eddy and swirl flow in the vapor box. However, in all cases, the footprint of MED-BVB has a 45% lower footprint compared to MED-SVB. Preference between configurations is subjected to the compromise between the operational challenges and site restrictions.

4. Conclusion

Steady state 2D and 3D CFD models were developed using COMSOL Multiphysics for two MED configurations namely MED-BVB and MED-SVB. The simulation was performed at different process recovery ratios with addressing

the effect of the number of demisters and demister orientation for both configurations.

The CFD results showed that, the conventional MED-BVB with one horizontal demister has 49% better vapor uniformity compared to the MED-SVB with three horizontal demisters. However, the MED-SVB with three inclined demisters configuration has 45% better vapor uniformity compared to the MED-BVB with one inclined demister. Generally, applying the proposed inclining demister showed a better uniform vapor flow in both configurations compared to conventional designs. Inclining the demister showed the superior of the MED-SVB configuration as it showed better vapor flow due to the wide passage resulted in less eddy and swirl flow in the vapor box. However, in all cases, the footprint of MED-BVB has a 45% lower footprint compared to MED-SVB. Preference between configurations is subjected to the compromise between the operational challenges and site restrictions. Finally, the future work will be focused on a novel MED internal design to overcome most of the MED desalination operational challenges specifically the thermal losses and vapor uniformity with compromising the system capex, footprint, and exergy.

References

- [1] IDA Desalination, Yearbook, Water Desalination Report, Media Analytics Ltd., UK, 2017–2018.
- [2] A. Mabrouk, H. Fath, Techno-economic study of a novel integrated thermal MSF-MED desalination technology, *Desalination*, 371 (2015) 115–125.
- [3] H.S. Son, M.W. Shahzad, N. Ghaffour, K.C. Ng, Pilot studies on synergetic impacts of energy utilization in hybrid desalination system: multi-effect distillation and adsorption cycle (MED-AD), *Desalination*, 477 (2020) 114266, doi: 10.1016/j.desal.2019.114266.
- [4] G. Ribatski, A.M. Jacobi, Falling film evaporation on horizontal tubes—a critical review, *Int. J. Refrig.*, 28 (2005) 635–653.
- [5] A.S. Nafey, M. Abdelkader, A. Abdelmotalip, A.A. Mabrouk, Enhancement of solar still productivity using floating perforated black plate, *Energy Convers. Manage.*, 43 (2002) 576–586.
- [6] J. Mitrovic, Preventing formation of dry patches in seawater falling film evaporators, *Desal. Water Treat.*, 29 (2011) 149–157.
- [7] F. Tahir, A. Mabrouk, M. Koc, Review on CFD analysis of horizontal falling film evaporators in multi effect desalination plants, *Desal. Water Treat.*, 166 (2019) 296–320.
- [8] F. Tahir, A. Mabrouk, M. Koc, Impact of surface tension and viscosity on falling film thickness in multi effect desalination (MED) horizontal tube evaporator, *Int. Therm. Eng.*, 150 (2019) 106235, doi: 10.1016/j.ijthermalsci.2019.106235.
- [9] J.J. Lorenz, D. Yung, E.N. Ganic, Vapor/liquid interaction and entrainment in falling film evaporators, *J. Heat Transfer*, 77 (1980) 69–73.
- [10] M.K. Mansour, M.A. Qassem, H. Fath, CFD analysis of vapor flow and design improvement in MED evaporation chamber, *Desal. Water Treat.*, 56 (2015) 2023–2036.
- [11] M.K. Mansour, H.E.S. Fath, Comparative study for different demister locations in multistage flash (MSF) flash chamber (FC), *Desal. Water Treat.*, 51 (2013) 7379–7393.
- [12] A. Mabrouk, A. Abotaleb, CFD analysis of the tube bundle orientation impact on the thermal losses and vapor uniformity within the MED desalination plant, *Desal. Water Treat.*, 143 (2019) 165–177.
- [13] A. Abotaleb, A. Mabrouk, CFD analysis of the demister location impact on the thermal losses and the vapor uniformity within the MED desalination plant, *Desal. Water Treat.*, 183 (2020) 42–53.
- [14] M. Ayala, P. Santos, G. Hamester, O. Ayala, Secondary Flow of Liquid-liquid Two-Phase Fluids in a Pipe Bend, Proceedings of the 2016 COMSOL Conference, Boston, MA, 2016.
- [15] N.G. Deen, M.S. Annal, J.A.M. Kuipers, Multi-scale modeling of dispersed gas–liquid two-phase flow, *Chem. Eng. Sci.*, 59 (2004) 1853–1861.
- [16] A.A. Mostafa, H.C. Mongia, On the modeling of turbulent evaporating sprays: Eulerian versus lagrangian approach, *Int. J. Heat Mass Transfer*, 30 (1987) 2583–2593.
- [17] T.H. Nigim, J.A. Eaton, CFD prediction of flashing processes in a MSF desalination chamber, *Desalination*, 420 (2017) 258–272.
- [18] A.S. Nafey, H.E.S. Fath, A.A. Mabrouk, A new visual package for design and simulation of desalination processes, *Desalination*, 194 (2006) 281–296.
- [19] A.S. Nafey, H. Fath, A.A. Mabrouk, Thermoeconomic investigation of multi effect evaporation (MEE) and hybrid multi effect evaporation-multi stage flash (MEE-MSF) systems, *Desalination*, 20 (2006) 241–254.
- [20] <http://hanbal.kr/pdf/hanbal>.